

Magneto-tunable terahertz absorption in single-layer graphene: A general approach

D. Jahani *, O. Akhavan, A. Alidoust Ghatar

June 22, 2022

Department of Physics, Sharif University of Technology, P.O. Box 11155-9161, Tehran, Iran
Leibniz Institute of Photonic Technology (IPHT), Jena, Germany.

Abstract

Terahertz (THz) anisotropic absorption in graphene could be significantly modified upon applying a static magnetic field on its ultra-fast 2D Dirac electrons. In general, by deriving the generalized Fresnel coefficients for monolayer graphene under applied magnetic field, relatively high anisotropic absorption for the incoming linearly polarized light with specific scattering angles could be achieved. We also prove that the light absorption of monolayer graphene corresponds well to its surface optical conductivity in the presence of a static magnetic field. Moreover, the temperature-dependent conductivity of graphene makes it possible to show that a step by step absorption feature would emerge at very low temperatures. We believe that these properties may be considered to be used in novel graphene-based THz application.

Keywords: Graphene; Terahertz light; Optical absorption; Magnetic field.

1 Introduction

The electromagnetic waves technology, especially in THz region ranging from 0.1 to 10 THz is of most interest in many fields and applications particularly in remote control, sensing and detectors which are mostly related to absorption properties of the material [1,2,3,4,5]. Moreover, materials that strongly interact with light giving appropriate and desirable responses in a broad range of frequencies play a critical role in science and technology such as, photonics security, photodetectors, sensors, photovoltaics and absorbers [6,7]. Therefore, existence of an material with high optical absorption in order to enhance absorption properties of structures could be the most desirable aim in applications. Isolated in 2004, graphene has shown to be one of the ideal materials in THz light absorption application [8].

Graphene, an atomic layer of carbons, has recently attracted enormous interest due to its exceptional electronic and optical properties [9,10,11]. Many researchers believe that graphene can be an appropriate substitute candidate for silicon in the next high-speed generation of photonic and electronic components, owing to its high carrier mobility, tunable optical conductivity, and uniform light absorption over a wide-band wavelength [12,13]. Graphene can absorb incoming beams in the range of different wavelengths from visible to infrared, while conventional semiconductors are unable to absorb

*d.jahani@sharif.edu

this range [14,15,16]. Bare graphene layer, owing to its unique band structure and massless carriers, approximately could absorb 2.3 percent of light [17,18,19]. Note that this amount of absorption is so impressive for a material with a 0.34 nm thickness. However, in general this amount of light absorption is considered to be very low and far from being used for desirable goals over a broad spectrum especially at the far-infrared and THz spectral ranges [17,20,21].

So far, several techniques have been introduced in order to enhance greatly the amount of light absorption of graphene in terms of theoretical and experimental approaches [22,23]. A long list of methods can be found in [20,21] for one that is interested to study which every method has its advantages and applications. Some methods are based on placing or embedding graphene in photonic crystals in order to achieve higher absorption [22,23,24,25]. Moreover, the optical absorption of graphene has been proved to be possible in a nanocavity resonator [26, 27]. Also perfect graphene absorber consisting of dielectric multilayer structures based on prism coupling has been reported [28,29,30]. Furthermore, it has been shown that, tuned by varying the Fermi level, a graphene-based absorber could be realized by a periodic double-layer graphene ribbon structure in infrared region [31]. However, no research proved the relatively high absorption of bare graphene by applying a static magnetic field in the quantum regime for which optical interband transitions and Landau levels (LLs) play a central role in light interaction with its massless Dirac electrons. Here, thanks again to the optical and electrical properties of graphene which can be tuned by external factors, we demonstrate that it is accessible to efficiently improve the absorption performance of bare graphene layer in the quantum Hall regime [32].

In this study, we aim to achieve multi- and broadband high light absorption in a bare graphene layer by applying a constant magnetic field since it could be so sufficient to be used in many optical applications. This paper is organized as follows: we discuss the model and calculating in section 2, then numerical calculations and results are addressed in section 3. In the end, we summarize our findings in section 4.

2 Structure and theoretical modeling

In this section, we provide a brief description of our calculation for incident s and p polarized light on a 2D conducting surface sandwiched between two dielectric media. In particular, we developed the components of the electric and magnetic vector of the incident, transmitted, and reflected waves as below [33]:

$$\begin{cases} E_i = (-a_p \cos \theta_i, a_s, a_p \sin \theta_i) e^{i\tau_i} \\ H_i Z_0 = (-a_s n_1 \cos \theta_i, -a_p n_1, a_s n_1 \sin \theta_i) e^{i\tau_i} \end{cases} \quad (1)$$

$$\begin{cases} E_r = (-r_p \cos \theta_r, r_s, r_p \sin \theta_r) e^{i\tau_r} \\ H_r Z_0 = (-r_s n_1 \cos \theta_r, -r_p n_1 e^{i\tau_r}, r_s n_1 \sin \theta_r) e^{i\tau_r} \end{cases} \quad (2)$$

$$\begin{cases} E_t = (-t_p \cos \theta_t, t_s e^{i\tau_t}, t_p \sin \theta_t) e^{i\tau_t} \\ H_t Z_0 = (-t_s n_2 \cos \theta_t, -t_p n_2 e^{i\tau_t}, t_s n_2 \sin \theta_t) e^{i\tau_t} \end{cases} \quad (3)$$

Here, a , r , and t are the complex amplitudes of the incidence, reflected, and transmitted waves with $\tau = \omega t - \mathbf{k} \cdot \mathbf{r}$. Then boundary conditions relate the electric and magnetic field components at the interface, $z = 0$ which can be described by following expressions::

$$\begin{cases} E_x^t = E_x^i + E_x^r & E_y^t = E_y^i + E_y^r, \\ H_x^t = H_x^i + H_x^r + J_y, & H_y^t = H_y^i + H_y^r - J_x \end{cases} \quad (4)$$

where $\mathbf{J} = \bar{\sigma} \cdot \mathbf{E}^t$. Here, \mathbf{J} and σ are the surface current density and the optical conductivity of 2D conducting material which we consider in to be graphene under an applied external magnetic field for which one can write the conductivity tensor as:

$$\sigma = \begin{pmatrix} \sigma_{xx} & \sigma_{xy} \\ \sigma_{yx} & \sigma_{yy} \end{pmatrix} = \begin{pmatrix} \sigma_0 & \sigma_H \\ -\sigma_H & \sigma_0 \end{pmatrix} \quad (5)$$

where σ_0 and σ_H , illustrate the longitudinal and Hall conductivity, respectively. By considering equations (2.1), (2.2), (2.3), (2.4) and the relation $\cos\theta_r = -\cos\theta_t$, reflection and transmission coefficients could be written in the following form:

$$\begin{cases} r_{ss} = \left(-1 + \frac{2n_1 G_1 \cos\theta_i}{G_1 G_2 - Z_0^2 \sigma_{yx} \sigma_{xy} \cos\theta_i \cos\theta_t}\right) \mathbf{a}_s, \\ r_{sp} = \left(\frac{2n_1 Z_0 \sigma_{yx} \cos\theta_i \cos\theta_t}{G_1 G_2 - Z_0^2 \sigma_{yx} \sigma_{xy} \cos\theta_i \cos\theta_t}\right) \mathbf{a}_p, \\ r_{pp} = \left(1 - \frac{2n_1 G_2 \cos\theta_t}{G_1 G_2 - Z_0^2 \sigma_{xy} \sigma_{yx} \cos\theta_i \cos\theta_t}\right) \mathbf{a}_p, \\ r_{ps} = \left(-\frac{2n_1 Z_0 \sigma_{xy} \cos\theta_i \cos\theta_t}{G_1 G_2 - Z_0^2 \sigma_{xy} \sigma_{yx} \cos\theta_i \cos\theta_t}\right) \mathbf{a}_s \end{cases} \quad (6)$$

$$\begin{cases} t_{ss} = \left(\frac{2n_1 G_1 \cos\theta_i}{G_1 G_2 - Z_0^2 \sigma_{yx} \sigma_{xy} \cos\theta_i \cos\theta_t}\right) \mathbf{a}_s, \\ t_{sp} = \left(\frac{2n_1 Z_0 \sigma_{yx} \cos\theta_i \cos\theta_t}{G_1 G_2 - Z_0^2 \sigma_{yx} \sigma_{xy} \cos\theta_i \cos\theta_t}\right) \mathbf{a}_p, \\ t_{pp} = \left(\frac{2n_1 G_2 \cos\theta_t}{G_1 G_2 - Z_0^2 \sigma_{xy} \sigma_{yx} \cos\theta_i \cos\theta_t}\right) \mathbf{a}_p, \\ t_{ps} = \left(\frac{2n_1 Z_0 \sigma_{xy} \cos^2\theta_i}{G_1 G_2 - Z_0^2 \sigma_{xy} \sigma_{yx} \cos\theta_i \cos\theta_t}\right) \mathbf{a}_s \end{cases} \quad (7)$$

where G_1 and G_2 are defined as $G_1 = n_1 \cos\theta_2 + n_2 \cos\theta_1 + Z_0 \sigma_{xx} \cos\theta_1 \cos\theta_2$ and $G_2 = n_1 \cos\theta_1 + n_2 \cos\theta_2 + Z_0 \sigma_{yy}$. Here, $Z_0 \approx 377\Omega$ is the vacuum impedance and \mathbf{a}_s (\mathbf{a}_p) is the amplitude of the electric vector of the incident field in the perpendicular (parallel) plane, respectively. Note that the subscripts of pp, ps and ss, sp indicate that incoming beams are linearly p- and s-polarized, respectively. However, pp, ps and ss, sp represent that the transmitted and reflect waves are p-, s- and s-, p- polarized, respectively. Now, as we use the quantum model for describing the conductivity, the longitudinal and Hall parts of the optical conductivity tensor (σ) of Dirac fermions with effective velocity V_f at the temperature T are as follows [34]:

$$\begin{aligned} \sigma_0(\omega) &= \frac{e^2 v_f^2 |eB| (\hbar\omega + 2i\Gamma)}{\pi i} \times \\ &\sum_{n=0}^{\infty} \left\{ \frac{[f_d(M_n) - f_d(M_{n+1})] + [f_d(-M_{n+1}) - f_d(-M_n)]}{(M_{n+1} - M_n)^3 - (\hbar\omega + 2i\Gamma)^2 (M_{n+1} - M_n)} \right\} \\ &+ \left\{ \frac{[f_d(-M_n) - f_d(M_{n+1})] + [f_d(-M_{n+1}) - f_d(M_n)]}{(M_{n+1} + M_n)^3 - (\hbar\omega + 2i\Gamma)^2 (M_{n+1} + M_n)} \right\} \end{aligned} \quad (8)$$

and:

$$\begin{aligned} \sigma_H(\omega) &= \frac{-e^2 v_f^2 eB}{\pi} \\ &\sum_{n=0}^{\infty} \{ [f_d(M_n) - f_d(M_{n+1})] - [f_d(-M_{n+1}) - f_d(-M_n)] \} \times \\ &\left\{ \frac{1}{(M_{n+1} - M_n)^2 - (\hbar\omega + 2i\Gamma)^2} + \frac{1}{(M_{n+1} + M_n)^2 - (\hbar\omega + 2i\Gamma)^2} \right\} \end{aligned} \quad (9)$$

in which $M_n = \sqrt{2n|eB|\hbar v_f^2}$. The scattering rate Γ is assumed to be independent of the light frequency and LLs index and the distribution function is $f_d(M_n = 1/(1 + \exp[(M_n - \mu)/K_B T])$ with e , \hbar and K_B representing electron charge and reduced Planck constant, Boltzmann constant, respectively. Finally, by the use of the above equations, the absorption of graphene for the incoming s/p-polarized light in quantum Hall regime could be given by:

$$A_{s/p} = 1 - (R_{ss}/pp + R_{ps}/sp + T_{ss}/pp + T_{ps}/sp) \quad (10)$$

3 Results and discussion

Our absorber structure is just based on a single-layer graphene under quantum Hall effect situation. However, as a matter of more illustration we also consider graphene layer to be on a dielectric substrate as it is demonstrated schematically in Fig.1. Here, the dielectric substrate is considered to be SiC (with the dielectric constant 4.4) on which graphene could be epitaxially grown with a controlled number of atomic layer l . First, in our simulations, we consider the incoming TE polarization (s-polarized) to obtain the absorption performance of graphene in a relatively low magnetic field for the proposed structure. We show the results in an energy interval ranging from 10 meV to 140 meV for the chemical potential 4 meV and Faraday geometry in which the external magnetic field is perpendicular to surface of graphene, i.e. along the propagation of incoming linearly polarized light (the case $\theta = 0$). It is clear from Fig.2 that graphene in the magnetic fields reveals a multi-band absorption performance. When the magnetic field is set to be $B = 1$ T and $B = 3$ T, the absorption of a graphene layer in the presence of a substrate has the amount of about 22% and 28.5% corresponding to the 76.53 meV and 132.6 meV photon energy, respectively. However, for bare graphene layer the absorption ratio is 42% and 49% for $B = 1$ T and $B = 3$ T, respectively. Now, if we take attention to the effective optical conductivity of graphene for the same parameters and $B = 1$ T, we see that boosting in absorption is directly related to the nature of the optical conductivity of graphene. In Fig. 3, We show the real and imaginary parts of the effective optical conductivity of graphene. As it is seen, each absorption peaks (for graphene with and without a substrate) in the energy position, exactly corresponding to the peaks of the optical conductivity of graphene. Consequently, this result indicates that the absorption performance of bare graphene could be tuned by modifying its optical conductivity.

The absorption of single-layer graphene under an increasing applying magnetic field for different angles of the incoming light for $\mu = 0.4$ eV and $E_{ph} = 20$ meV at a very low temperature $T = 1$ K and the room temperature $T = 300$ K is depicted in Fig. 4. We, in Fig. 4 (a), observe a step-like scheme emerges for the absorption of graphene as a function of the magnetic field ranging from $B = 1$ T to $B = 50$ T. It is clear that by increasing the magnetic field the absorption is also increased until it reaches its ultimate amount. Then this trend is reversed and the absorption falls gradually by increasing the field. In Fig. 4 (b) the role of scattering angle in the absorption is more clear. Note that, as it is clear from Fig. 4 (c) at a higher temperature the absorption will be boosted to some extent and the step-like scheme tends to vanish. The situation is more illustrated in Fig.4 (d).

In the following, the effect of the chemical potential ranging from $\mu = 0.1$ eV to $\mu = 0.8$ eV on the absorption performance on graphene has been surveyed. The outcomes are illustrated as a function of the angle of the incidence of incoming linearly polarized light and also two different temperatures. For graphene with a substrate ($E_{ph} = 20$ meV and $B = 20$ T) similar to the magnetic field case, a plateau-like shape for the absorption can be seen (Fig. 5 (a)). The absorption is increased step

by step until about $\mu = 0.471$ eV, then it begins to fall. Note that, in spite of the fact that the highest plateau has happened in the chemical potential between 0.471 eV and 0.511 eV, the maximum absorption is occurred at $\mu = 0.491$ eV with 19.38% at $\theta = 0$. From Fig. 5(c) it is clear that enlarging angle of the incoming light leads to the lower absorption for graphene. Besides, at high temperatures, the absorption rate is boosted up to 21.19% and the step-like structure, as it might be expected, also tends to be faded. In Fig. 6, the absorption versus the chemical potential for graphene without a substrate in a similar condition as indicated in Fig. 5, have been examined. In comparison to Fig. 5, the step-like situation is also taking place and the absorption is increased by increasing the chemical potential.

At this point, to see how the photon energy (E_{ph}) ranging from 0.1 meV to 70 meV affects the absorption of graphene, we also examine it as a function of the incident angles at $B = 20$ T and $\mu = 0.4$ eV for $T = 1$ K and $T = 300$ K. For graphene layer as it is observed from Fig. 7(a), the absorption of incoming s-polarized light shows a peak at a specific angle. Therefore, we see that A_s increases when the direction of the applied magnetic field makes an angle to the propagation of the incident light relative to the Faraday geometry for a specific light's scattering angle. However, the absorption of the incoming p-polarized incident light increasing by increasing the scattering angle leads to lower values for A_p (see Fig. 8).

4 Conclusion

In summery, we investigated the absorption spectrum of intraband and interband transitions through the surface conductivity tensor of graphene in its general anisotropic state. We have numerically detailed the optical absorption of single layer graphene in THz region with and without a substrate (SiC) under quantum Hall effect situation. Since, in general, the initial polarization of light will no be preserved under the presence of the magnetic field, we have examined the effect of increasing the static magnetic field, chemical potential and photon energy interval for different incident angles of the incoming linearly polarized light. It was shown that any peak in the absorption performance of graphene layer in the photon energy interval directly corresponds to the enhancement of the optical conductivity of monolayer graphene. Therefore, we see that enhancement of the absorption of bare graphene is directly related to the profile of the optical conductivity of graphene. However, one can use photonic resonates and other resonance methods to increase the absorption of graphene-based devices. Significantly, applying a magnetic field on garpehene results in appearing a step-like scheme in the absorption of graphene at low temperatures. Moreover, we proved that higher absorption for bare graphene can be achieved for special incident angles of incident light relative to the Faraday geometry which may open opportunities for further investigation of light absorption in graphene-based THz application.

5 Data availability

Data sharing is not applicable to this article as no new data were created or analyzed in this study.

References

- [1] *J. Lloyd-Hughes, J. Faist, H. E. Beere, D. A. Ritchie, L. Sirbu, I. M. Tiginyanu, S. K. M. Merchant and M. B. Johnston. Terahertz conductivity of magnetoexcitons and electrons in semi-*

conductor nanostructures. *Ultrafast Phenomena in Semiconductors and Nanostructure Materials XIII*. Vol. 7214. SPIE, 2009.

- [2] J. Federici, L. Moeller. Review of terahertz and subterahertz wireless communications, *J. Appl. Phys.* 107 (11) (2010) 6 (2010).
- [3] P.U. Jepsen, D.G. Cooke, M. Koch, Terahertz spectroscopy and imaging-Modern techniques and applications, *Laser Photon. Rev.* 5 (1) 124-166 (2011).
- [4] Z. Wei, Y. Jiang, S. Zhang, X. Zhu, and Q. Li. Graphene-Based Magnetically Tunable Broadband Terahertz Absorber. *IEEE Photonics Journal*, 14(1), 1-6 (2021).
- [5] M. Tonouchi. Cutting-edge terahertz technology. *Nature photonics*, 1(2), 97-105 (2007).
- [6] J. Zhang, S. Cao, and L. Guan. Carbon monoxide gas sensor based on cavity enhanced absorption spectroscopy and harmonic detection. *2009 Symposium on Photonics and Optoelectronics (pp. 1-4)*. IEEE.
- [7] C. M. Watts, X. Liu, and W. J. Padilla. Metamaterial electromagnetic wave absorbers (*adv. mater.* 23/2012). *Advanced Materials*, 24(23), OP181-OP181 (2012).
- [8]B. Sensale-Rodriguez, R. Yan, M. M. Kelly, T. Fang, K. Tahy, W. S. Hwang, D. Jena, L. Liu and H. G. Xing. Broadband graphene terahertz modulators enabled by intraband transitions. *Nature communications*, 3(1), 1-7 (2012).
- [9] A. C. Neto, F. Guinea, N.M. Peres, K.S. Novoselov, A.K. Geim, The electronic properties of graphene, *Rev. Modern Phys.* 81 (1)109 (2009).
- [10] A. K. Geim, K.S. Novoselov, The rise of graphene. *Nat. Mater*, 6(3), 183-191 (2007).
- [11] L. A. Falkovsky. Optical properties of graphene. *ournal of Physics: conference series*. Vol. 129. No. 1. IOP Publishing, (2008).
- [12] H. Yang, Y. Wang, Z. C. Tiu, S. J. Tan, L. Yuan, and H. Zhang. All-Optical Modulation Technology Based on 2D Layered Materials. *Micromachines*, 13(1), 92 (2022).
- [13] C. C. Lee, S. Suzuki, W. Xie, and T. R. Schibli. Broadband graphene electro-optic modulators with sub-wavelength thickness. *Optics express*, 20(5), 5264-5269 (2012).
- [14] H. Yang, Y. Wang, Z. C. Tiu, S. J. Tan, L. Yuan, and H. Zhang. All-Optical Modulation Technology Based on 2D Layered Materials. *Micromachines*, 13(1), 92 (2022).
- [15] A. Nematpour, N. Lisi, L. Lancellotti, R. Chierchia, and M. L. Grilli. Experimental Mid-Infrared Absorption (84%) of Single-Layer Graphene in a Reflective Asymmetric Fabry-Perot Filter: Implications for Photodetectors. *ACS Applied Nano Materials*, 4(2), 1495-1502 (2021).
- [16] M. Grande, M. A. Vincenti, T. Stomeo, G. V. Bianco, D. De Ceglia, N. Akozbek, V. Petruzzelli, G. Bruno, M. De Vittorio, M. Scalora, and A. D'Orazio. Graphene-based perfect optical absorbers harnessing guided mode resonances. *Optics Express*, 23(16), 21032-21042 (2015).

- [17] R. R. Nair, P. Blake, A. N. Grigorenko, K. S. Novoselov, T. J. Booth, T. Stauber, N. M. R. Peres, and A. K. Geim. *Fine structure constant defines visual transparency of graphene*. *Science*, 320(5881), 1308-1308 (2008).
- [18] J. M. Dawlaty, S. Shivaraman, J. Strait, P. George, M. Chandrashekar, F. Rana, M. G. Spencer, D. Veksler, and Y. Chen. *Measurement of the optical absorption spectra of epitaxial graphene from terahertz to visible*. *Applied Physics Letters*, 93(13), 131905 (2008).
- [19] S. Cao, Q. Wang, X. Gao, S. Zhang, R. Hong, and D. Zhang. *Monolayer-Graphene-Based Tunable Absorber in the Near-Infrared*. *Micromachines*, 12(11), 1320 (2021)..
- [20] S. Lee, H. Heo, and S. Kim. *Graphene perfect absorber of ultra-wide bandwidth based on wavelength-insensitive phase matching in prism coupling*. *Scientific reports*, 9(1), 1-9 (2019).
- [21] B. Liu, C. Tang, J. Chen, N. Xie, H. Tang, X. Zhu, and G. S. Park. *Multiband and broadband absorption enhancement of monolayer graphene at optical frequencies from multiple magnetic dipole resonances in metamaterials*. *Nanoscale research letters*, 13(1), 1-7 (2018)
- [22] Z. Wu, B. Xu, M. Yan, B. Wu, Z. Sun, P. Cheng, X. Tong, and S. Ruan. *Broadband microwave absorber with a double-split ring structure*. *Plasmonics*, 15, 1863-1867 (2020).
- [23] H. S. Lee, J. Y. Kwak, T. Y. Seong, G. W. Hwang, W. M. Kim, I. Kim, and K. S. Lee. *Optimization of tunable guided-mode resonance filter based on refractive index modulation of graphene*. *Scientific reports*, 9(1), 1-11 (2019).
- [24] J. D. Joannopoulos, S. G. Johnson, J. N. Winn, and R. D. Meade. *Molding the flow of light*. Princeton Univ. Press, Princeton, NJ [ua] (2008).
- [25] X. Wang, X. Jiang, Q. You, J. Guo, X. Dai, and Y. Xiang, Y. *Tunable and multichannel terahertz perfect absorber due to Tamm surface plasmons with graphene*. *Photonics Research*, 5(6), 536-542 (2017).
- [26] *Aperiodic perforated graphene in optical nanocavity absorbers*, S Bidmeshkipour, O Akhavan, P Salami, L Yousefi, *Materials Science and Engineering: B* 276 115557 (2022).
- [27] Bidmeshkipour, Samina, and Omid Akhavan. "Graphene Nanopores in Broadband Wide-Angle Optical Cavity Resonance Absorbers." *Surfaces and Interfaces* (2022): 101956.
- [28] S. Lee, and S. Kim. "Practical perfect absorption in monolayer graphene by prism coupling." *IEEE Photonics Journal* 9.5: 1-10 (2017).
- [29] Q. Ye, J. Wang, Z. Liu, Z. C. Deng, X. T. Kong, F. Xing, X. D. Chen, W. Y. Zhou, C. P. Zhang, and J. G. Tian. *Polarization-dependent optical absorption of graphene under total internal reflection*. *Applied Physics Letters*, 102(2), 021912 (2013).
- [30] T. Okamoto, M. Yamamoto, and I. Yamaguchi, (2000). *Optical waveguide absorption sensor using a single coupling prism*. *JOSA A*, 17(10), 1880-1886.
- [31] H. Li, L. Wang, and X. Zhai. *Tunable graphene-based mid-infrared plasmonic wide-angle narrowband perfect absorber*. *Scientific reports*, 6(1), 1-8 (2016).

- [32] M. Wang, Y. Wang, M. Pu, C. Hu, X. Wu, Z. Zhao, and X. Luo, X. Circular dichroism of graphene-based absorber in static magnetic field. *Journal of Applied Physics*, 115(15), 154312 (2014).
- [33] M. Born and E. Wolf, *Principles of Optics*, 6th ed. (Cambridge University Press, Cambridge, 1980).
- [34] V. P. Gusynin, S. G., Sharapov, and J. P. Carbotte. Magneto-optical conductivity in graphene. *Journal of Physics: Condensed Matter*, 19(2), 026222 (2006).

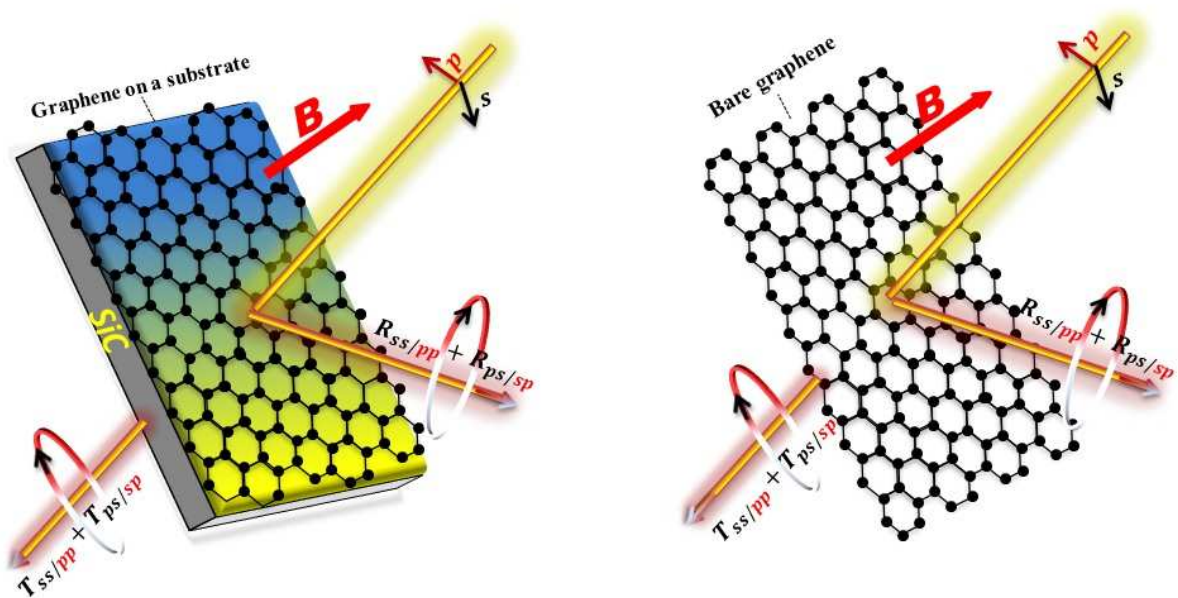


Figure 1: Schematic representation of light's incidence on graphene in a general non-Faraday geometry (the perpendicular external magnetic field applied on the surface of graphene is not along the propagation of the incident light).

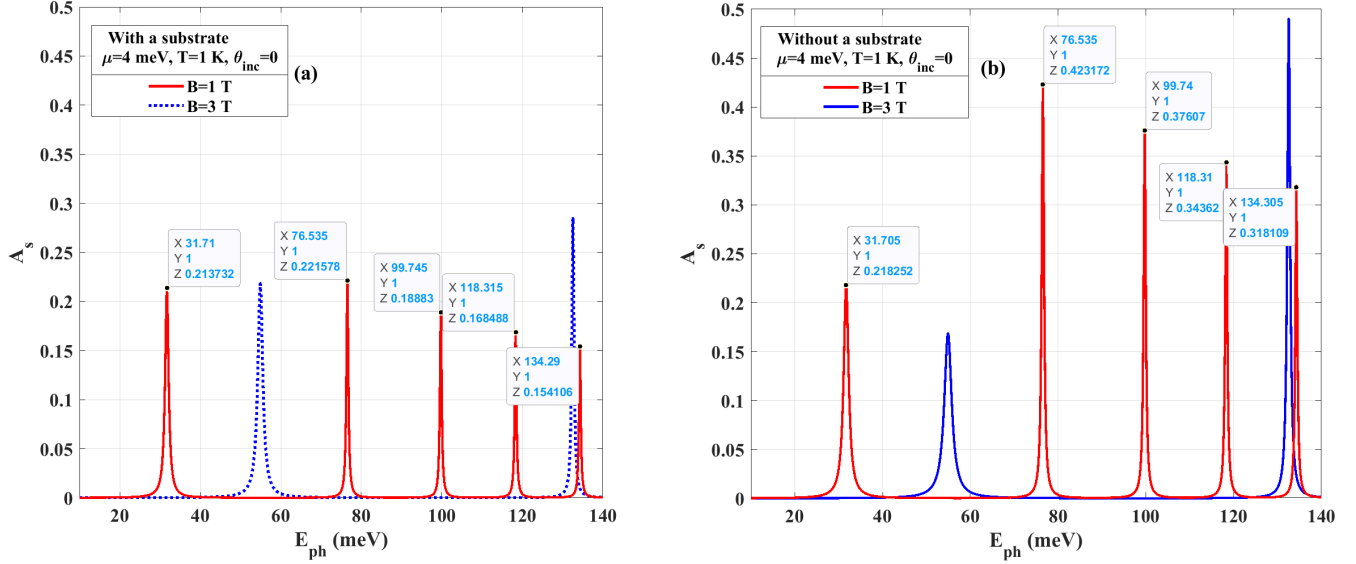


Figure 2: (a) Absorption of bare graphene versus the photon energy interval ranging from 0.1 meV to 140 meV for $B = 1$ T (red curve) and $B = 3$ T (Blue curve) at $T = 1$ K for the incident light. (b) Absorption of graphene on SiC versus the photon energy. We see that absorption for bare graphene could mark higher values than the case when it is put on a substrate.

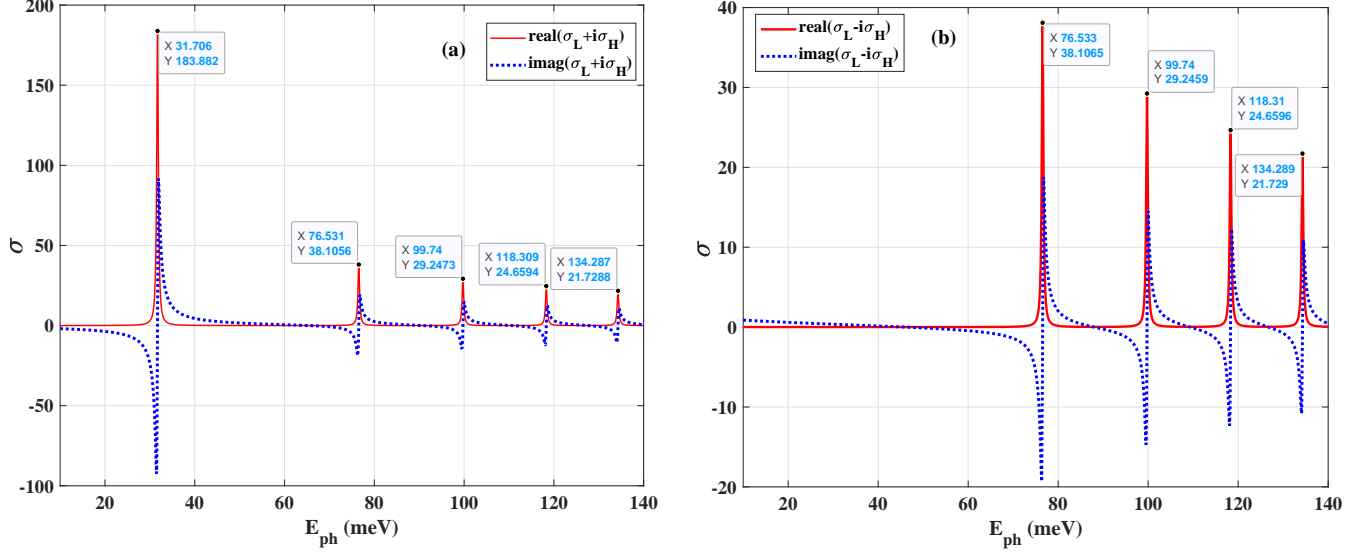


Figure 3: (a) and (b) The real and imaginary part of effective conductivity as a function of the photon energy E_{ph} with the parameters used as in Fig.2 for left and right handed waves. As it is clear, the peaks in the optical conductivity exactly correspond to the peaks seen in the absorption.

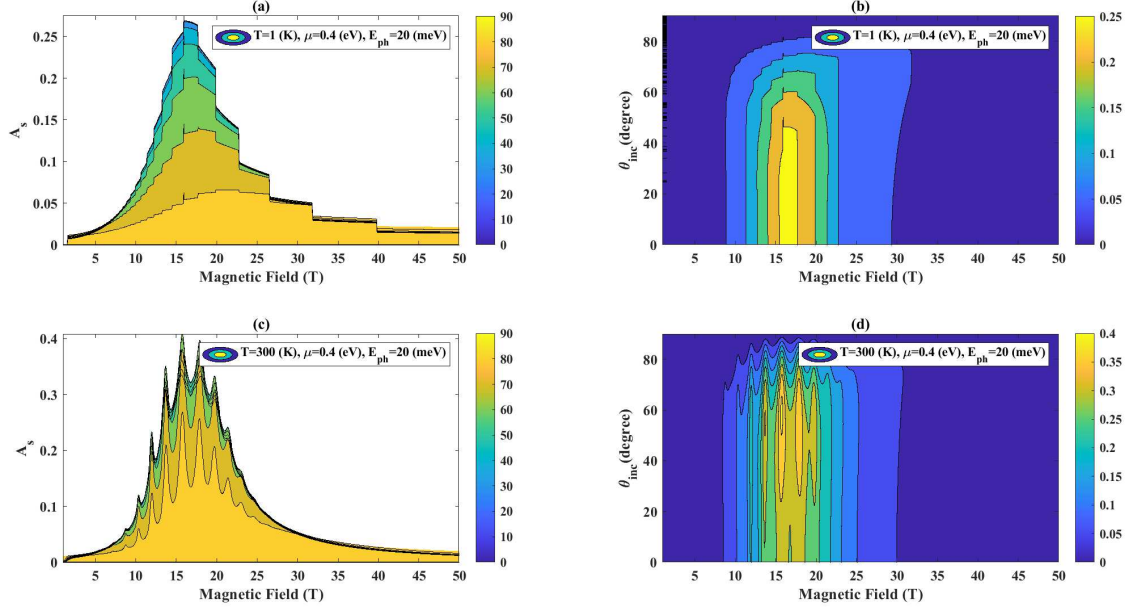


Figure 4: (a) and (b) Absorption spectra under the effect of increasing magnetic field for different incident angles of incoming s-polarized THz light at $T = 1$ K. (c) and (d) Absorption at the high temperature ($T = 300$ K) for graphene. As it is expected, a step-like scheme for the absorption appears at low temperatures. However, when the temperature increases the step-like feature vanishes. The absorption for higher incident angles shows to be increased for s-polarized light.

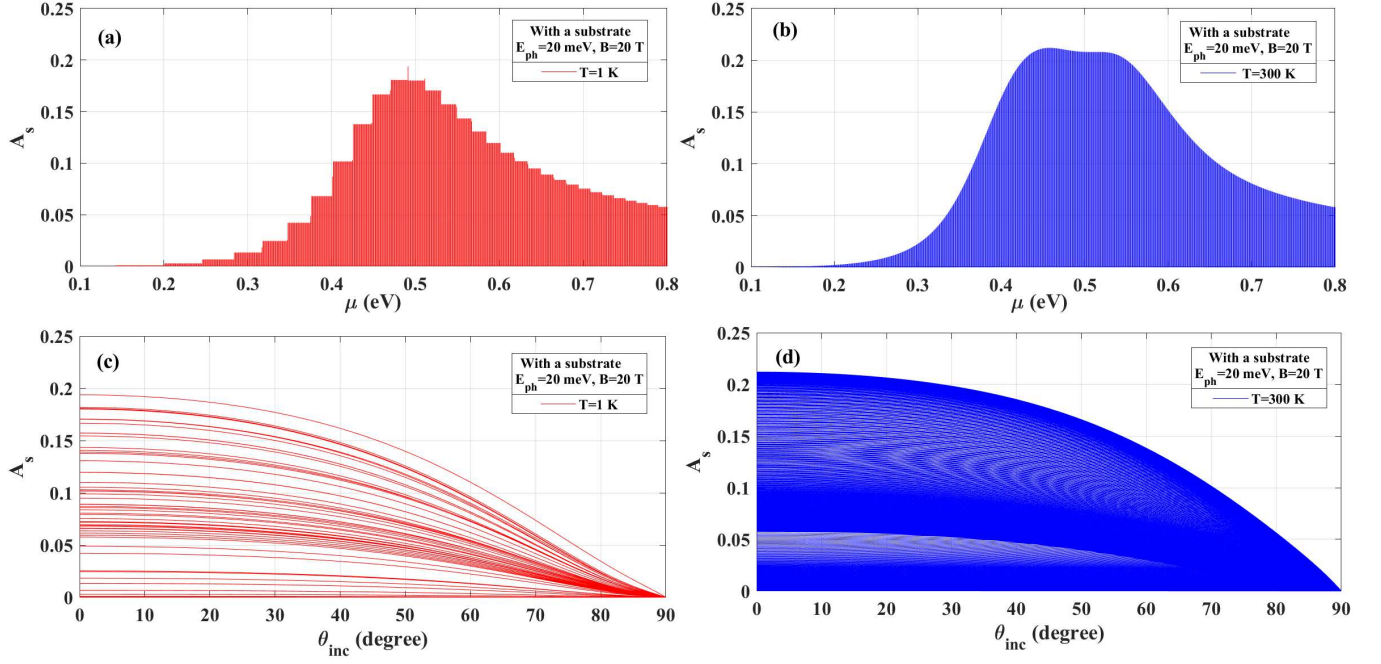


Figure 5: Variation in the absorption versus the chemical potential at $T = 1$ K (a) and $T = 300$ K (b) for graphene on SiC. Absorption as a function of the incident angle at $T = 1$ K (c) and $T = 300$ K (d) for graphene with a substrate for $E_{ph} = 20$ meV and $B = 20$ T.

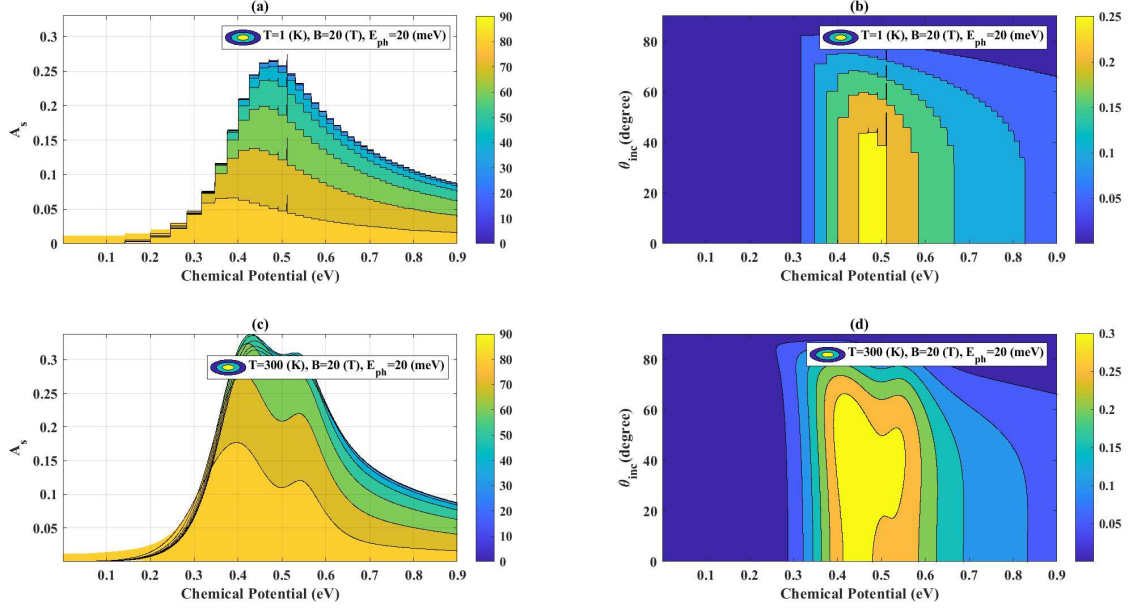


Figure 6: (a) and (b) Absorption of bare graphene as a function of the chemical potential for $T = 1$ K. (c) and (d) Impact of incoming light for different scattering angles at $T = 300$ K for bare graphene under the incident s-polarized light with $E_{ph} = 20$ meV and $B = 20$ T.

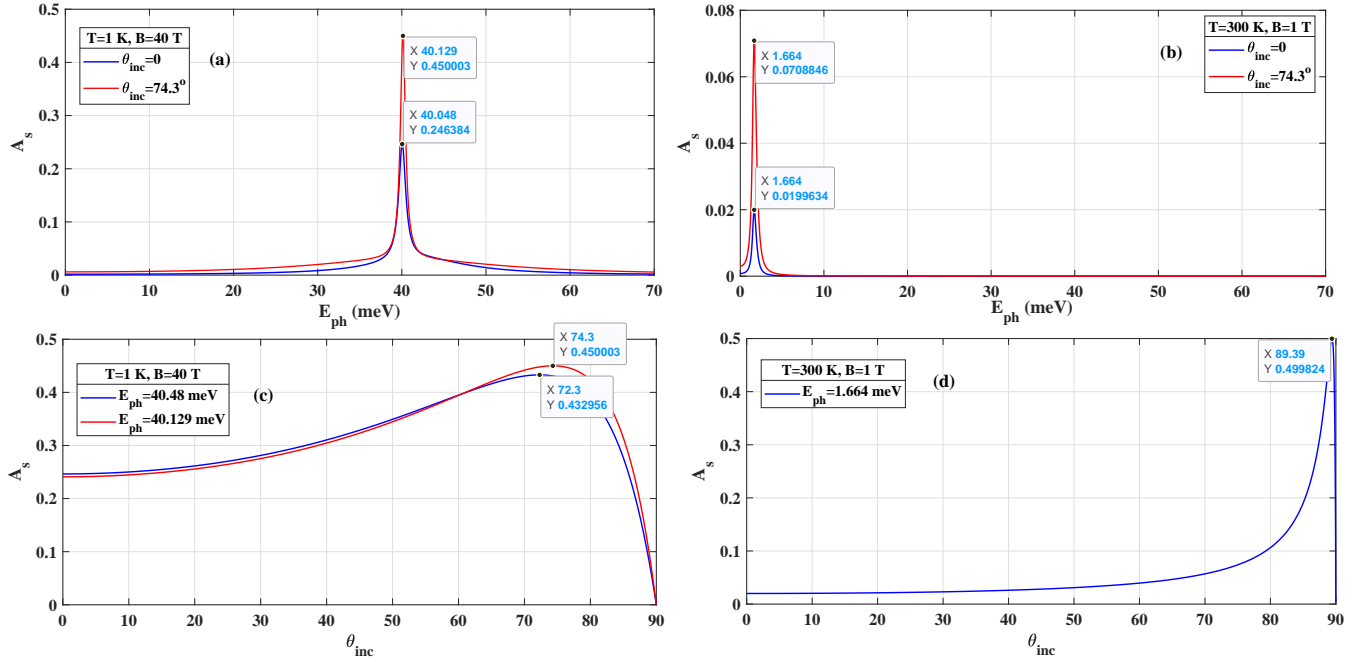


Figure 7: (a) and (b) Absorption for two different scattering angle at $T = 1\text{ K}$ and $T = 300\text{ K}$, respectively. Absorption for different scattering angles at $T = 1\text{ K}$ (c) and $T = 300\text{ K}$ (d) for bare graphene for two different values for photon energy with s polarization.

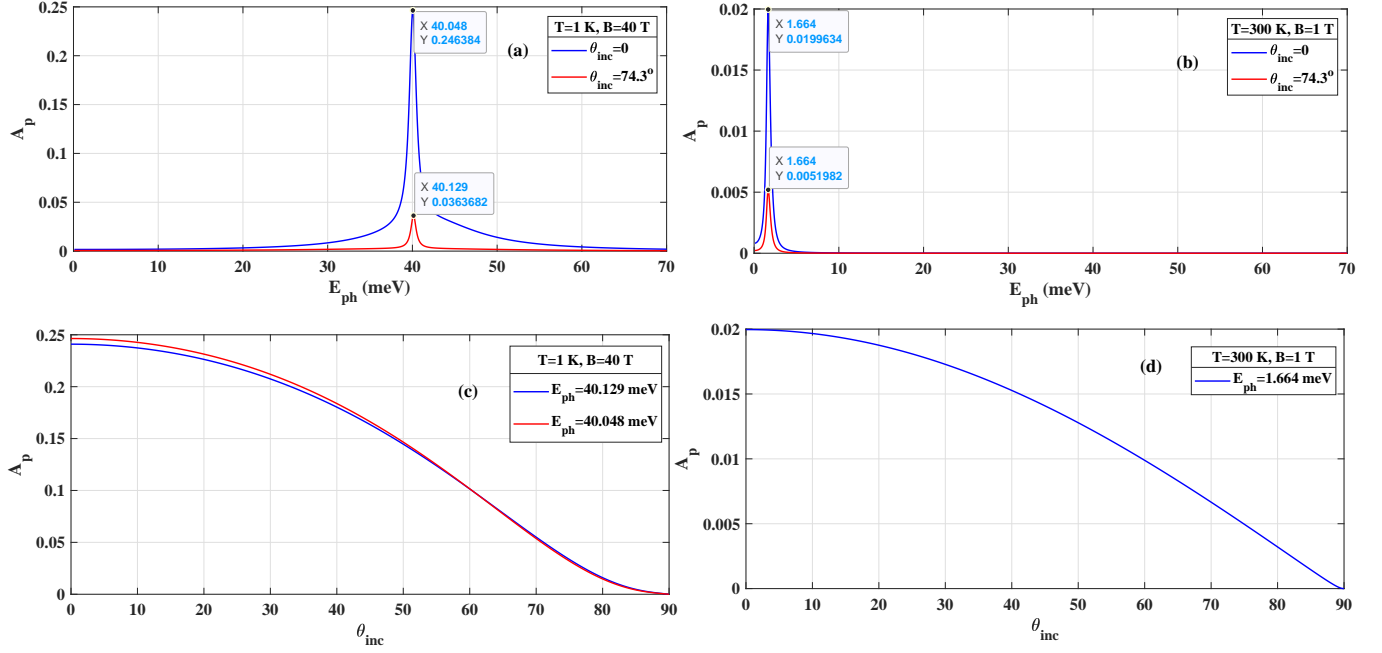


Figure 8: (a) and (b) Absorption of incoming p-polarized light at $T = 1$ K and $T = 300$ K, respectively. Impact of incoming light in different angles at $T = 1$ K (c) and $T = 300$ K (d) for bare graphene for two different values for photon energy with s polarization .